

REPORT

***Hmga1* null mouse embryonic fibroblasts display downregulation of spindle assembly checkpoint gene expression associated to nuclear and karyotypic abnormalities**

Giovanna Maria Pierantoni^{a,†}, Andrea Conte^{a,†}, Cinzia Rinaldo^b, Mara Tornincasa^a, Raffaele Gerlini^a, Davide Valente^b, Antonella Izzo^a, and Alfredo Fusco^a

^aIstituto di Endocrinologia ed Oncologia Sperimentale del CNR and Dipartimento di Medicina Molecolare e Biotecnologie Mediche, Università di Napoli “Federico II”, Naples, Italy; ^bIstituto di Biologia e Patologie Molecolari del CNR c/o Università “Sapienza” di Roma, Rome, Italy

ABSTRACT

The High Mobility Group A1 proteins (HMGA1) are nonhistone chromatinic proteins with a critical role in development and cancer. We have recently reported that HMGA1 proteins are able to increase the expression of spindle assembly checkpoint (SAC) genes, thus impairing SAC function and causing chromosomal instability in cancer cells. Moreover, we found a significant correlation between HMGA1 and SAC genes expression in human colon carcinomas. Here, we report that mouse embryonic fibroblasts null for the *Hmga1* gene show downregulation of *Bub1*, *Bub1b*, *Mad2l1* and *Ttk* SAC genes, and present several features of chromosomal instability, such as nuclear abnormalities, binucleation, micronuclei and karyotypic alterations. Interestingly, also MEFs carrying only one impaired *Hmga1* allele present karyotypic alterations. These results indicate that HMGA1 proteins regulate SAC genes expression and, thereby, genomic stability also in embryonic cells.

ARTICLE HISTORY

Received 6 July 2015
Revised 5 January 2016
Accepted 20 January 2016

KEYWORDS

Chromosome instability;
HMGA1; SAC

Introduction

The High Mobility Group A1 (HMGA1) gene codes for 2 proteins, HMGA1a and HMGA1b, through alternative splicing.¹ These proteins are nonhistone architectural nuclear factors, able to bind the minor groove of AT-rich DNA sequences through 3 “AT-hook” domains. HMGA1 proteins are abundantly expressed during embryonic development, and at low levels in normal adult tissues.^{2–3} Conversely, HMGA overexpression is a feature of malignant neoplasias.⁴

Impairment of the HMGA1 expression causes cardiac hypertrophy and diabetes, indicating a critical role of these proteins in cardiomyocytic growth regulation⁵ and glucose metabolism.⁶

We have recently demonstrated that HMGA1 positively regulates the transcription of *Bub1*, *Bub1b*, *Mad2l1* and *Mps1/Ttk* genes involved in the spindle assembly checkpoint (SAC) by binding to their promoters, and that HMGA1 overexpression compromises the mitotic checkpoint activity leading to chromosome instability. Moreover, we have reported that human colon carcinomas and their liver metastasis show high SAC gene expression that correlates with HMGA1 protein levels.⁷

Here, we have investigated the effects of the lack of HMGA1 protein on SAC gene expression and genomic stability in mouse embryonic fibroblasts (MEFs) null for the *Hmga1* gene. We found that *Hmga1* null MEFs present downregulation of SAC gene expression associated to nuclear abnormalities, micronuclei, binucleation and aberrant karyotypes.

Results

***Bub1*, *Bub1b*, *Mad2l1* and *Ttk* expression is downregulated in *Hmga1*^{-/-} MEFs**

We have previously reported that HMGA1 proteins bind *Bub1*, *Bub1b*, *Mad2l1* and *Ttk* promoters and positively regulate their transcriptional activity in NIH3T3 and colon cancer cells.

Since these genes are involved in the regulation of the cell cycle⁸ in MEFs, we have evaluated *Bub1*, *Bub1b*, *Mad2l1* and *Ttk* expression by qRT-PCR and western blotting in *Hmga1*^{+/+} and *Hmga1*^{-/-} MEFs. As shown in Fig. 1A and 1B, all these genes were significantly downregulated in *Hmga1*^{-/-} MEFs, compared to the corresponding wild-type (WT) cells. The restoration of *Hmga1* expression in the *Hmga1* null MEFs through the transfection of pcDNA3.1-*Hmga1b* vector induces a strong increase in *Bub1*, *Bub1b*, *Mad2l1* and *Ttk* transcript levels, that was not observed in the same cells transfected with the control vector (CV) (Fig. 1C).

Therefore, these results indicate that HMGA1 positively regulates *Bub1*, *Bub1b*, *Mad2l1* and *Ttk* genes also in MEFs, suggesting that the HMGA1-mediated regulation of these genes may occur also during embryogenesis.

***Hmga1* null MEFs display nuclear abnormalities, micronuclei and binucleation**

It has been previously shown that the deregulation of key SAC genes, obtained by *Mad2l1* overexpression or *Bub1b*^{+/-} mice, is

CONTACT Alfredo Fusco ✉ alfusco@unina.it; Giovanna Maria Pierantoni ✉ gmpieran@unina.it ✉ Department of Molecular Medicine and Medical Biotechnology, University of Naples “Federico II”, Via Pansini 5 80131 Naples, Italy.

Color versions of one or more of the figures in this article can be found online at www.tandfonline.com/kccy.

[†]These authors equally contributed to this work.

© 2016 Taylor & Francis

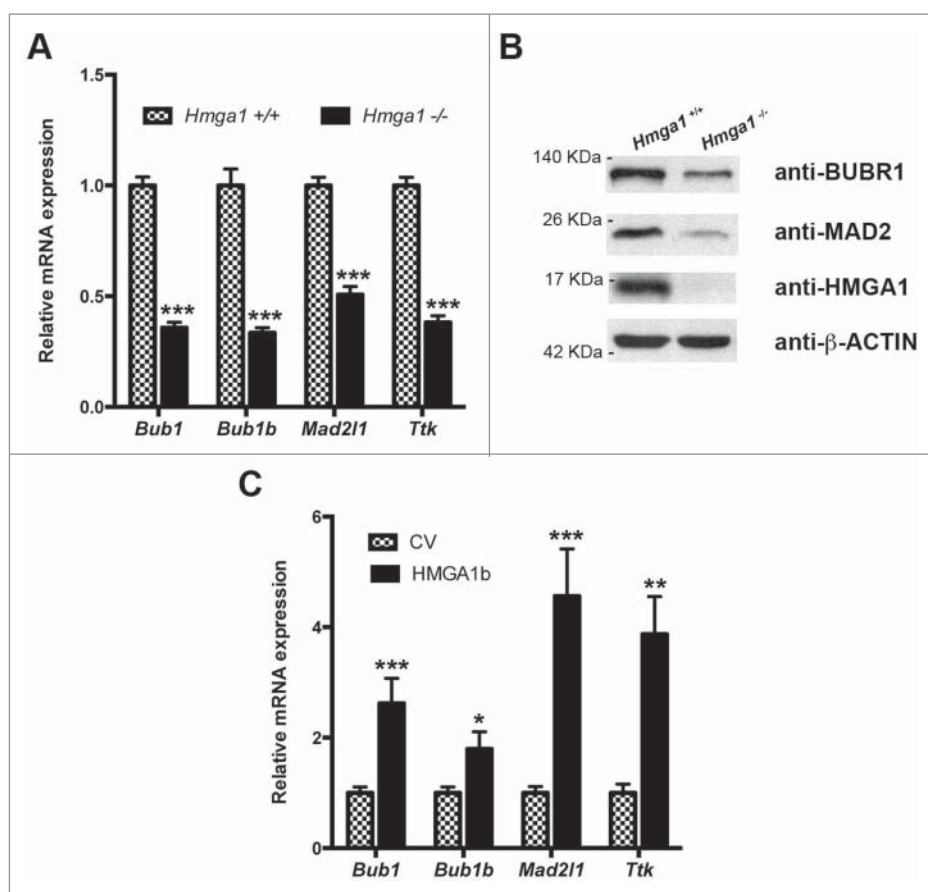


Figure 1. HMGA1 modulates *Bub1*, *Bub1b*, *Mad211* and *Ttk* mRNA expression levels in MEFs. RNA and proteins extracted from *Hmga1*^{+/+} and *Hmga1*^{-/-} MEFs were analyzed by qRT-PCR for *Bub1*, *Bub1b*, *Mad211* and *Ttk* expression (A) and by western blotting using the indicated antibodies (B). The actin expression level has been used for data normalization. qRT-PCR values are mean \pm SD of a representative experiment performed in triplicate. (C) RNA extracted from *Hmga1*^{-/-} MEFs transiently transfected with empty vector (CV) or pcDNA3.1-*Hmga1b* expression vector was analyzed by qRT-PCR for *Bub1*, *Bub1b*, *Mad211* and *Ttk* expression. Values are mean \pm SD of a representative experiment performed in triplicate.

often associated with nuclear division or cytokinesis impairment, resulting in the formation of polyploid cells frequently accompanied by micronuclei.^{9,10} This prompted us to evaluate the presence of nuclear abnormalities in *Hmga1*^{-/-} MEFs examining the nuclear features of *Hmga1*^{+/+} and *Hmga1*^{-/-} MEFs at several culture passages. At early passage (passage 3; p3), 12.2 ± 2.4 % of the *Hmga1*^{-/-} MEFs exhibit binuclear phenotype compared with 2.4 ± 0.56 % of the *Hmga1*^{+/+} MEFs. These differences were also observed at later passages (p6) with 13.1 ± 2.3 % binucleated cells of the *Hmga1*^{-/-} MEFs compared with 4.05 ± 2.73 % of the *Hmga1*^{+/+} MEFs (Fig. 2A). In addition, the percentage of cells having more than 2 nuclei was elevated in the *Hmga1*^{-/-} MEFs, with 2.00 ± 0.29 % and 4.11 ± 0.87 at the p3 and p6, respectively, with respect to the 0.49 ± 0.27 % and 1.80 ± 0.57 % of the *Hmga1*^{+/+} at the same passages. Interestingly, we observed also a trend toward a time-dependent accumulation of cells exhibiting micronucleation and/or aberrantly-shaped nuclei (i.e. bi- and multilobated large nuclei) that represent typical features of chromosome instability (indicated as micronucleated and aberrant cells in Fig. 2A). In the Fig. 2B-C, representative images of *Hmga1*^{+/+} and *Hmga1*^{-/-} MEFs at the p3 and p6 are shown. Moreover, as already reported⁸ and as suggested by the observation of MEFs in culture (Fig. 2C), we found that the growth rate of *Hmga1*^{-/-} MEFs was much lower than that of the WT counterpart (Fig. 2D).

To further confirm the correlation between lack of HMGA1 and nuclear abnormalities in MEFs, we examined the nuclear features of MEFs after HMGA1-silencing. To this aim, MEFs were transfected with siRNAs targeting the *Hmga1* gene (*Hmga1i* cells) or with control siRNA (*Ctli* cells). Consistently with the data shown above, HMGA1-silencing reduced SAC gene expression (*Bub1*, *Bub1b*, *Mad211* and *Ttk*), as shown by qRT-PCR analysis (Fig. 3A). Then, the immunofluorescence analysis showed an increased number of binucleated cells (21%) in the *Hmga1i* in comparison with the *Ctli* cells (13%) (Fig. 3B-C).

Overall, these findings strongly support the hypothesis that the downregulation of key SAC genes observed in HMGA1 depleted MEFs results in nuclear phenotypes that can be due to chromosome segregation defects and/or cytokinesis failure associated to CIN.

Karyotypic alterations in *Hmga1*^{-/-} and *Hmga1*^{+/-} MEFs

Subsequently, we analyzed the karyotype of *Hmga1*^{+/+} and *Hmga1*^{-/-} MEFs since the deregulation of one or more SAC proteins can induce the impairment of checkpoint, thereby resulting in genomic instability. This analysis has been

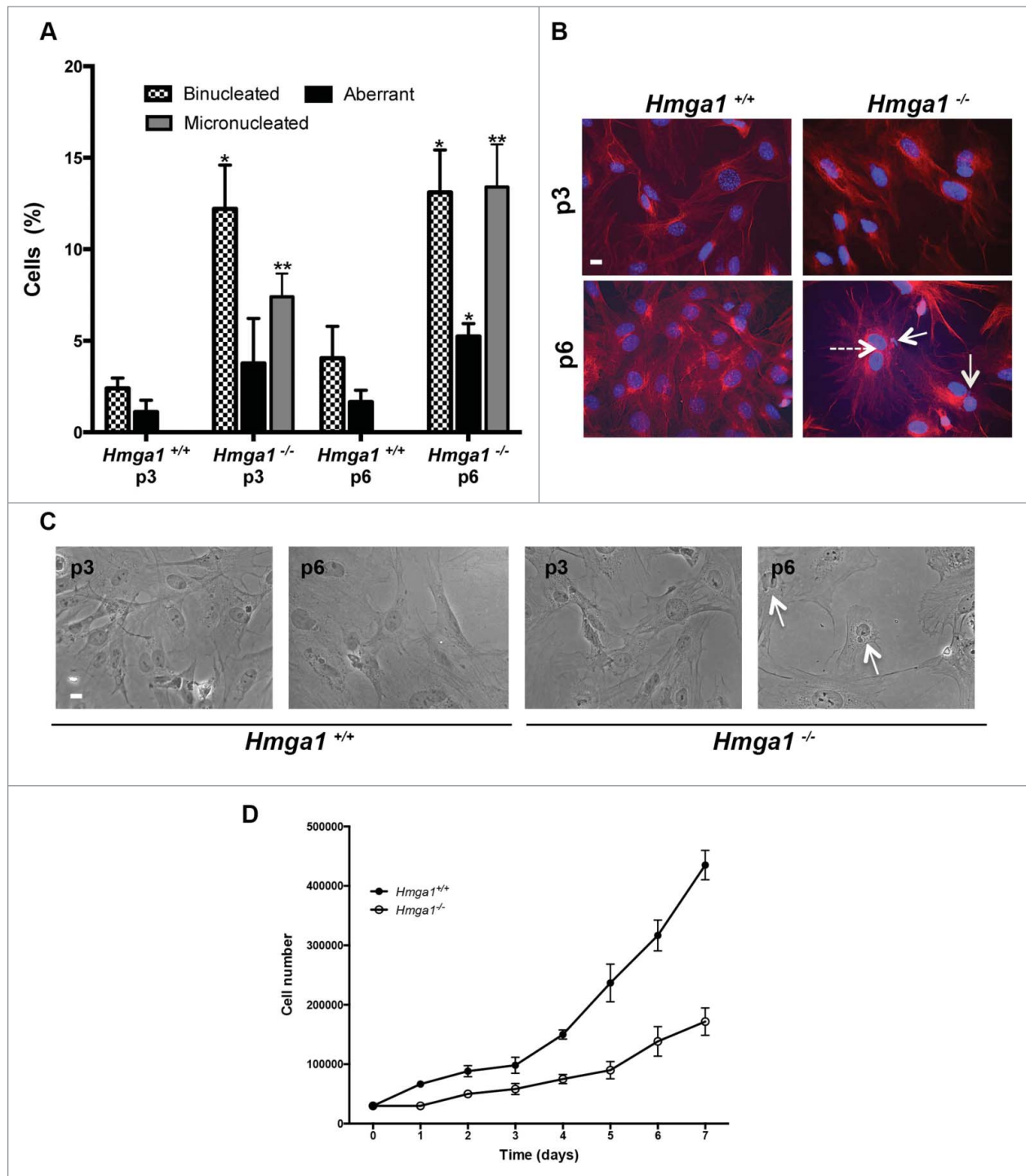


Figure 2. Lack of HMG1 expression induces nuclear abnormalities, micronuclei and binucleation. (A) *Hmga1*^{+/+} and *Hmga1*^{-/-} MEFs were stained with DAPI and anti- β -tubulin antibody to identify the nuclei and the cytoplasm, respectively. About 1,000 cells *per* sample were scored for the presence of aberrantly-shaped nuclei, micronuclei and for the presence of one or 2 nuclei/cell. The data are represented as mean SD. Differences between *Hmga1*^{+/+} and *Hmga1*^{-/-} are statistically significant: ** $p < 0.01$ for micronucleated, and * $p < 0.05$ for binucleated cells and aberrant cells, $n = 3$ independent experiments. (B-C) Representative fields of *Hmga1*^{+/+} and *Hmga1*^{-/-} cells at p3 and p6. Staining with anti- β -tubulin antibody and DAPI (B); brightfield (C). Dashed arrows indicate binucleated cells. Solid arrows indicate micronuclei. Scale bar, 10 μ m. (D) Proliferation rate of *Hmga1*^{+/+} and *Hmga1*^{-/-} MEFs at culture passage 3. Cells were plated and counted daily for 7 d. Values represent mean \pm SEM.

conducted on cells at different culture passages since chromosomal alterations could accumulate with the round of mitoses.

To analyze the karyotype of the *Hmga1*^{+/+} and *Hmga1*^{-/-} MEFs, the cells have been plated on cover-slides, and after 24 hours, they have been incubated with colcemid to arrest mitosis and then treated as described in Material and methods. At passage 3 a high percentage (23%) of *Hmga1* null MEFs

were tetraploid, and a little amount of cells (about 9%) presented 160 chromosomes, whereas only 37% showed a normal karyotype. At p6, we found a higher number of cells (30%) with 160 chromosomes with respect to p3, whereas the number of *Hmga1*^{-/-} MEFs showing normal karyotype decreased to 25%. Furthermore, about 31% of *Hmga1*^{-/-} cells shows an aberrant number of chromosomes not multiple of 40 at

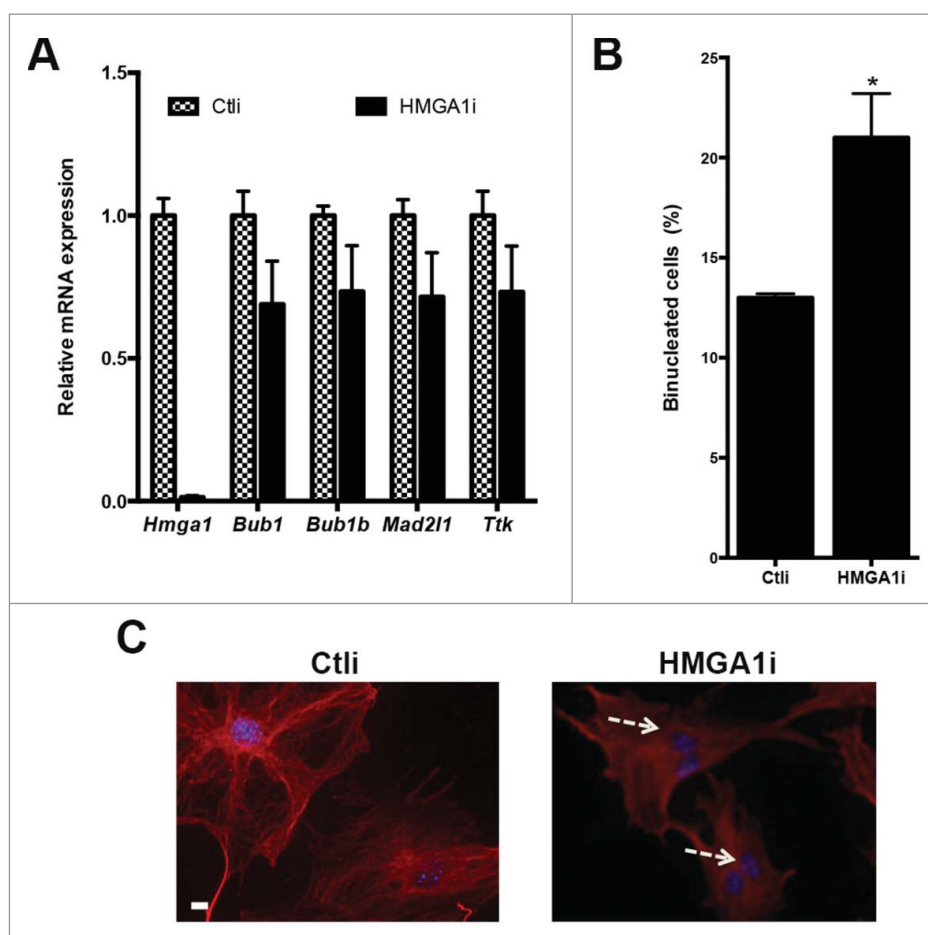


Figure 3. Down-regulation of HMGA1 by RNAi induces binucleation in MEFs. (A) Control (Ctl) and HMGA1-depleted (HMGA1i) WT MEFs were tested for the expression of HMGA1 and SAC genes by qPCR 72 hours post transfection. The actin expression level has been used for data normalization. qRT-PCR values are mean \pm SD of a representative experiment performed in triplicate. (B) As described in "Materials and Methods" section, after 2 rounds of transfection, Ctl and HMGA1i MEFs were stained with DAPI and anti- β -tubulin antibody to identify the nuclei and the cytoplasm, respectively. About 1,000 cells *per* sample were scored for the presence of binucleated cells. The data are represented as mean \pm SD. Differences between Ctl and HMGA1i MEFs are statistically significant for binucleated cells ($*p < 0.05$). (C) Representative fields of Ctl and HMGA1i MEFs, staining with anti- β -tubulin antibody and DAPI. Dashed arrows indicates binucleated cells. Scale bar, 10 μ m.

passages 3 and 6, with a percentage about 31% at p3 and about 25% at p6. Conversely, WT MEFs showed 8% and 15% of tetraploidy at p3 and p6, respectively, and no cells with aberrant number of chromosomes (Fig. 4A). Furthermore, we analyzed the karyotype of the *Hmga1*^{+/-} cells, and we observed that 72% of the heterozygous MEFs showed a normal karyotype, 24% an aneuploid karyotype and only 4% of these MEFs were tetraploid at p3. At p6, only about 50% of the *Hmga1*^{+/-} MEFs presented normal karyotype, whereas the other cells showed mostly an aneuploid karyotype (Fig. 4A-B).

In conclusion, *Hmga1*^{-/-} and *Hmga1*^{+/-} MEFs have a considerable higher percentage of cells with tetraploid and abnormal karyotype compared to *Hmga1*^{+/+} MEFs, indicating that HMGA1 complete or partial depletion leads to tetra-/polyploidization and aneuploidization.

Discussion

In this study we report that genetic ablation of *Hmga1* gene in MEFs, that physiologically express HMGA1 protein at high levels, causes downregulation of *Bub1*, *Bub1b*, *Mad2l1* and *Ttk* SAC genes. These data are consistent with those

previously published, showing that HMGA1 overexpression induces SAC gene upregulation in HCT116 and NIH3T3 cells⁷.

The downregulation of SAC genes observed in HMGA1 null MEFs results in micronucleation and/or aberrantly-shaped nuclei, that can be due to chromosome segregation defects and cytokinesis failure, which are common features of CIN associated to SAC impairment (Fig. 2). These alterations, associated with a considerable higher percentage of cells with tetraploid and abnormal karyotypes, accumulate with the round of mitoses, indicating that HMGA1 depletion induces chromosomal instability (Fig. 4). Interestingly, karyotypic abnormalities are already present in absence of only one *Hmga1* allele. Moreover, in heterozygous MEFs, these alterations consist mainly in gain or loss of one or few chromosomes, whereas the homozygous null MEFs (*Hmga1*^{-/-}) are characterized by a higher grade of polyploidy. The high percentage of polyploidy in *Hmga1*^{-/-} MEFs suggests that HMGA1 may play an important role in the maintenance of genomic stability, not only regulating SAC genes expression, but also through other mechanisms, such as the control of cytokinesis.

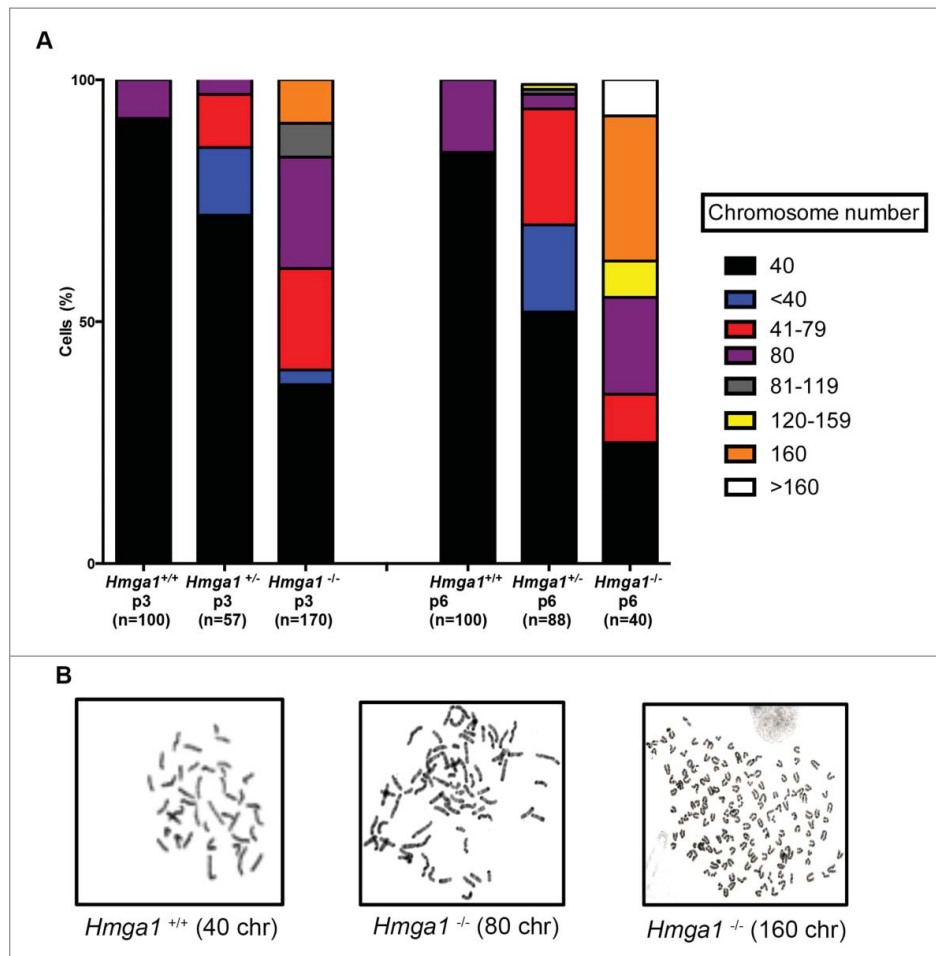


Figure 4. Lack of HMGA1 expression induces karyotypic alterations. (A) The graph shows the percentages of *Hmga1*^{+/+}, *Hmga1*^{+/-} and *Hmga1*^{-/-} MEFs with the indicated chromosome number at two different culture passages (p3 and p6). The number of analyzed metaphases for each sample has been indicated. (B) Representative images of karyotypes of indicated MEFs with different chromosome number.

The presence of chromosomal abnormalities in *Hmga1* null MEFs could seem in contrast with the viability of the *Hmga1*^{-/-} mice. However, it is likely that the presence of chromosomal abnormalities becomes more evident *in vitro* than *in vivo*, where they could be compensated by some unknown mechanisms. Moreover, we can also hypothesize that *Hmga1*^{-/-} MEFs accumulate less aneuploidy *in vivo* because they undergo a lower number of proliferation rounds.

Therefore, these results confirm a critical role of the HMGA1 proteins in regulating the expression of SAC genes, and the role of these genes in regulating chromosomal stability. Consistently, it has been reported that mice carrying conditional *Bub1* mutation develop severe defects ranging from early lethality to tumorigenesis.¹¹ It has also been demonstrated that the SAC works only when all its components are expressed at “optimal” levels. In fact, there are many evidences that either an upregulation or downregulation of one or more SAC genes, that frequently occur in cancer cells, may impair the checkpoint and cause CIN, thus playing an important role in cancer progression.¹²⁻¹⁹ Moreover, SAC gene de-regulation has been related also to chemoresistance to anti-microtubule drugs in several cancer types.²⁰⁻²³

In conclusion, the results reported here and in our previous study⁷ suggest that HMGA1 regulating SAC genes expression contributes to the maintainance of genomic stability in embryonic

cells, whereas its overexpression, a feature of malignant neoplasias, contributes to cancer progression, inducing chromosomal instability that eventually leads to a more advanced cancer status.

Materials and methods

Cell cultures, transfections and plasmids

MEFs were cultured in DMEM with 10% FBS, L-glutamine, and antibiotics (Invitrogen, Carlsbad, CA). The restoration of *Hmga1* expression in the *Hmga1*^{-/-} MEFs was obtained with the transfection of pcDNA3.1-*Hmga1b* vector using the NeonTM Transfection System. Cells were electroporated under the following conditions: Pulse voltage (v): 1350, Pulse Width (ms): 30, Pulse number: 1. RNA interference was obtained by HMGA1-specific mix of 3 different siRNAs [Qiagen Mm_HMGA1_2, Mm_HMGA1_3, Mm_HMGA1_6 (SI02672901, SI02693201, SI05380921)] using Lipofectamine RNAi MAX (Invitrogen), according to manufacturer’s instructions. Qiagen AllStars control siRNA (SI03650318) was used as negative control. 72 hours post the first round of transfection, cells were collected, re-plated and re-transfected as above described. 48 hours after the second round of transfection, cells were analyzed by immunofluorescence.

Growth curve

MEFs were plated in triplicate in a series of 6-cm culture dishes and counted daily with a cell counter for 7 consecutive days to perform growth curves. The values represent means \pm SEM.

Protein extraction, western blotting, and antibodies

Cells were lysed in lysis buffer containing 1% NP40, 1 mM EDTA, 50 mM Tris-HCl (pH 7.5) and 150 mM NaCl, supplemented with complete protease inhibitors mixture (Roche Branford, CT, USA). Total proteins were separated by SDS-polyacrylamide gel electrophoresis and transferred to nitrocellulose membranes (Amersham, Rainham, UK) by electroblotting.²⁴ Membranes were blocked with 5% non-fat dry milk and incubated with antibodies anti-actin (sc-1616, Santa Cruz Biotechnology), anti-HMGA1,²⁵ anti-BUBR1 (612503, BD Transduction Laboratories), anti-MAD2 (610678, Transduction Laboratories).

MEF isolation and genotyping

All mice were maintained under standardized non-barrier conditions in the animal facility of DMMBM, and all studies were conducted in accordance with Italian regulations for experiments on animals. MEFs have been isolated from 12.5 d.p.c. embryos. After head removing, embryos have been washed with PBS, incubated in trypsin 1% (Sigma) for 10 minutes at RT, pelleted and then resuspended in DMEM. MEFs have been genotyped for HMGA1 by PCR analysis with the following primers:

HMGA1-Fw 5'-AGAGACAAGAATGGGAGAGC-3'
 HMGA1wt-Re 5'-TGTTACTAGGACCCTCATGG-3'
 HMGA1KO-Re 5'-TAAAGCGACTGCTCCAGACT-3'

The wild-type allele is amplified using HMGA1-Fw + HMGA1wt-Re primers, while the knock-out allele is amplified using HMGA1-Fw + HMGA1KO-Re primers.

RNA extraction and quantitative Real Time PCR (qRT-PCR)

Total RNA was isolated using TRI-reagent solution (Sigma, St Louis, MO, USA) and treated with DNase (Invitrogen). Reverse transcription was performed according to standard procedures (Qiagen, Valencia, CA). qRT-PCR analysis for *Bub1*, *Bub1b*, *Mad211*, and *Ttk* was performed using the Power SYBR Green PCR Master Mix (Applied Biosystems) according to manufacturers' instructions with following primer sequences:

mouseBub1-Fw 5'-CAAGGACCTTCCTGCTTCTG-3'
 mouseBub1-Re5'-GACTTGGACCCCTCAATTCC-3'
 mouseBub1b-Fw5'-GCCAGATTGCAGATTGCTTC-3'
 mouseBub1b-Re 5'-GGACAGATGGAACAGGACAG-3'
 mouseTtk-Fw 5'-ATATGGCCCCAGAAGCAATC-3'
 mouseTtk-Re 5'-CCCCAAGGACCAGACATCAC-3'
 mouseMad211-Fw 5'-AGAAACTGGTGGTGGTCATC-3'
 mouseMad211-Re 5'-CGAACACCTTCCTCTTTTGC-3'
 mouseHmga1-Fw 5'-CAAGACCCGGGAAAGTCA-3'
 mouseHmga1-Re 5'-CAGAGGACTCCTGGGAGATG-3'
 mouseActin-Fw 5'-CTAAGGCCAACCGTGAAAAG-3'
 mouseActin-Re 5'-ACCAGAGGCATACAGGGACA-3'

To calculate the relative expression levels we used the 2- $\Delta\Delta$ CT method.²⁶ Primers specific for the actin were used for normalization of Real-Time quantitative PCR data.

Karyotype analysis

Cells have been plated on cover-slides and, after 24 hours, they have been treated as previously described.²⁷ Metaphase spreads have been stained with Giemsa (Sigma) according to standard procedures. 100 metaphases from wild-type MEFs at passages 3 and 6 were analyzed; 170 metaphases and 40 metaphases from *Hmga1* null MEFs were analyzed at passages 3 and 6, respectively; 57 metaphases and 88 metaphases from *Hmga1* heterozygous MEFs were analyzed at passages 3 and 6, respectively. Slides were hybridized by spectral karyotyping. Images were acquired with Mac Ktype 5.6 on Olympus BX61 microscope with a Zeiss optical filter (magnification 100X).

Immunofluorescence

Cells plated on cover-slides in 12 wells plates were fixed in 4% formaldehyde in PBS and permeabilized in a solution of 0.25% Triton X-100 in PBS. To analyze the percentage of mono-, bi-, multi- and micro-nucleated cells immunofluorescence was performed with anti β -tubulin antibody conjugated to CY3 (Sigma) and stained with DAPI to identify the cytoplasm and the nuclei, respectively. Cells were observed with a fluorescent microscope (Zeiss, magnification 63X or 100X).

Statistical analysis

Student's t-test was used to determine the significance for all the quantitative experiments. Error bars represent the standard deviation (SD) of the average.

Abbreviations

Bub1	budding uninhibited by benzimidazoles 1
CIN	chromosome instability
HMGA1	high mobility group A1
MEF	mouse embryo fibroblasts
Mad211	mitotic arrest deficient-like 1
SAC	spindle assembly checkpoint

Disclosure of potential conflicts of interest

No potential conflicts of interest were disclosed.

Acknowledgments

We are grateful to Mr. L. Di Guida from DMMBM for technical support. Mara Tornincasa was recipient of a fellowship from Fondazione Italiana per la Ricerca sul Cancro (FIRC).

Funding

This work was supported by grants (IG-11477, MFAG-11702 and IG-17739) from the Associazione Italiana Ricerca sul Cancro (AIRC), from Ministero Salute-Giovani Ricercatori, PNR-CNR Aging "Program 2012-2014."

References

- [1] Johnson KR, Lehn DA, Reeves R. Alternative processing of mRNAs encoding mammalian chromosomal high-mobility-group proteins HMG-I and HMG-Y. *Mol Cell Biol* 1989; 9(5):2114-23; PMID:2701943; <http://dx.doi.org/10.1128/MCB.9.5.2114>
- [2] Chiappetta G, Avantiaggiato V, Visconti R, Fedele M, Battista S, Trappasso F, Merciai BM, Fidanza V, Giancotti V, Santoro M, et al. High level expression of the HMGI (Y) gene during embryonic development. *Oncogene* 1996; 13(11):2439-46; PMID:8957086
- [3] Zhou X, Benson KF, Ashar HR, Chada K. Mutation responsible for the mouse pygmy phenotype in the developmentally regulated factor HMGI-C. *Nature* 1995; 376(6543):771-4; PMID:7651535; <http://dx.doi.org/10.1038/376771a0>
- [4] Fusco A, Fedele M. Roles of HMGA proteins in cancer. *Nat Rev Cancer* 2007; 7(12):899-910. Review; PMID:18004397; <http://dx.doi.org/10.1038/nrc2271>
- [5] Fedele M, Fidanza V, Battista S, Pentimalli F, Klein-Szanto AJ, Visone R, De Martino I, Curcio A, Morisco C, Del Vecchio L, et al. Haploinsufficiency of the Hmgal1 gene causes cardiac hypertrophy and myelo-lymphoproliferative disorders in mice. *Cancer Res* 2006; 66(5):2536-43; PMID:16510570; <http://dx.doi.org/10.1158/0008-5472.CAN-05-1889>
- [6] Foti D, Chiefari E, Fedele M, Iuliano R, Brunetti L, Paonessa F, Manfioletti G, Barbetti F, Brunetti A, Croce CM, et al. Lack of the architectural factor HMGA1 causes insulin resistance and diabetes in humans and mice. *Nat Med* 2005; 11(7):765-73; PMID:15924147; <http://dx.doi.org/10.1038/nm1254>
- [7] Pierantoni GM, Conte A, Rinaldo C, Tornincasa M, Gerlini R, Federico A, Valente D, Medico E, Fusco A. Deregulation of HMGA1 expression induces chromosome instability through regulation of spindle assembly checkpoint genes. *Oncotarget* 2015; 6(19):17342-53; PMID:26009897.
- [8] Federico A, Forzati F, Esposito F, Arra C, Palma G, Barbieri A, Palmieri D, Fedele M, Pierantoni GM, De Martino I, Fusco A. Hmgal1/Hmgal2 double knock-out mice display a "superpygmy" phenotype. *Biol Open* 2014; 3(5):372-8; PMID:24728959; <http://dx.doi.org/10.1242/bio.20146759>
- [9] Sotillo R, Hernando E, Díaz-Rodríguez E, Teruya-Feldstein J, Cordon-Cardo C, Lowe SW, Benezra R. Mad2 overexpression promotes aneuploidy and tumorigenesis in mice. *Cancer Cell* 2007; 11(1):9-23; PMID:17189715; <http://dx.doi.org/10.1016/j.ccr.2006.10.019>
- [10] Wang Q, Liu T, Fang Y, Xie S, Huang X, Mahmood R, Ramaswamy G, Sakamoto KM, Darzynkiewicz Z, Xu M, Dai W. BUBR1 deficiency results in abnormal megakaryopoiesis. *Blood* 2004; 103(4):1278-85; PMID:14576056; <http://dx.doi.org/10.1182/blood-2003-06-2158>
- [11] Schliekelman M, Cowley DO, O'Quinn R, Oliver TG, Lu L, Salmon ED, Van Dyke T. Impaired Bub1 function in vivo compromises tension-dependent checkpoint function leading to aneuploidy and tumorigenesis. *Cancer Res* 2009; 69(1):45-54; PMID:19117986; <http://dx.doi.org/10.1158/0008-5472.CAN-07-6330>
- [12] Ricke RM, van Deursen JM. Aurora B hyperactivation by Bub1 overexpression promotes chromosome missegregation. *Cell Cycle* 2011; 10(21):3645-51; PMID:22033440; <http://dx.doi.org/10.4161/cc.10.21.18156>
- [13] Lin SF, Lin PM, Yang MC, Liu TC, Chang JG, Sue YC, Chen TP. Expression of hBUB1 in acute myeloid leukemia. *Leuk Lymphoma* 2002; 43:385-91; PMID:11999574; <http://dx.doi.org/10.1080/10428190290006206>
- [14] Alizadeh AA, Eisen MB, Davis RE, Ma C, Lossos IS, Rosenwald A, Boldrick JC, Sabet H, Tran T, Yu X, et al. Distinct types of diffuse large B-cell lymphoma identified by gene expression profiling. *Nature* 2000; 403:503-11; PMID:10676951; <http://dx.doi.org/10.1038/35000501>
- [15] van't Veer LJ, Dai H, van de Vijver MJ, He YD, Hart AA, Mao M, Peterse HL, van der Kooy K, Marton MJ, Witteveen AT, et al. Gene expression profiling predicts clinical outcome of breast cancer. *Nature* 2002; 415:530-6; PMID:11823860; <http://dx.doi.org/10.1038/415530a>
- [16] Grabsch H, Takeno S, Parsons WJ, Pomjanski N, Boecking A, Gabbert HE, Mueller W. Overexpression of the mitotic checkpoint genes BUB1, BUBR1, and BUB3 in gastric cancer-association with tumour cell proliferation. *J. Pathol* 2003; 200:16-22; PMID:12692836; <http://dx.doi.org/10.1002/path.1324>
- [17] Shigeishi H, Oue N, Kuniyasu H, Wakikawa A, Yokozaki H, Ishikawa T, Yasui W. Expression of Bub1 gene correlates with tumor proliferating activity in human gastric carcinomas. *Pathobiology* 2001; 69:24-29; PMID:11641614; <http://dx.doi.org/10.1159/000048754>
- [18] Kops GJ, Weaver BA, Cleveland DW. On the road to cancer: aneuploidy and the mitotic checkpoint. *Nat Rev Cancer* 2005; 5:773-85; PMID:16195750; <http://dx.doi.org/10.1038/nrc1714>
- [19] Gordon DJ, Resio B, Pellman D. Causes and consequences of aneuploidy in cancer. *Nat Rev Genet* 2012; 13:189-203; PMID:22269907
- [20] Bargiela-Iparraguirre J, Prado-Marchal L, Pajuelo-Lozano N, Jiménez B, Perona R, Sánchez-Pérez I. Mad2 and BubR1 modulates tumorigenesis and paclitaxel response in MKN45 gastric cancer cells. *Cell Cycle* 2014; 13(22):3590-601; PMID:25483095; <http://dx.doi.org/10.4161/15384101.2014.962952>
- [21] Hu M, Liu Q, Song P, Zhan X, Luo M, Liu C, Yang D, Cai Y, Zhang F, Jiang F, et al. Abnormal expression of the mitotic checkpoint protein BubR1 contributes to the anti-microtubule drug resistance of esophageal squamous cell carcinoma cells. *Oncol Rep* 2013; 29(1):185-92; PMID:23128493
- [22] McGrogan BT, Gilmartin B, Carney DN, McCann A. Taxanes, microtubules and chemoresistant breast cancer. *Biochim Biophys Acta* 2008; 1785(2):96-132
- [23] Chanel-Vos C, Giannakakou P. CENP-E checks in microtubule-drug resistance. *Cell Cycle* 2010; 9(8):1456; PMID:20421712; <http://dx.doi.org/10.4161/cc.9.8.11382>
- [24] Esposito F, Tornincasa M, Chieffi P, De Martino I, Pierantoni GM, Fusco A. High-mobility group A1 proteins regulate p53-mediated transcription of Bcl-2 gene. *Cancer Res* 2010; 70(13):5379-88; PMID:20530667; <http://dx.doi.org/10.1158/0008-5472.CAN-09-4199>
- [25] Pierantoni GM, Battista S, Pentimalli F, Fedele M, Visone R, Federico A, Santoro M, Viglietto G, Fusco A. A truncated HMGA1 gene induces proliferation of the 3T3-L1 pre-adipocytic cells: a model of human lipomas. *Carcinogenesis* 2003; 24(12):1861-9; PMID:12970064; <http://dx.doi.org/10.1093/carcin/bgg149>
- [26] Livak KJ, Schmittgen TD. Analysis of relative gene expression data using real-time quantitative PCR and the 2⁻(Delta Delta C(T)) Method. *Methods* 2001; 25(4):402-8; PMID:11846609; <http://dx.doi.org/10.1006/meth.2001.1262>
- [27] Valente D, Bossi G, Moncada A, Tornincasa M, Indelicato S, Piscuoglio S, Karamitopoulou ED, Bartolazzi A, Pierantoni GM, Fusco A, et al. HIPK2 deficiency causes chromosomal instability by cytokinesis failure and increases tumorigenicity. *Oncotarget* 2015; 6(12):10320-34; PMID:25868975; <http://dx.doi.org/10.18632/oncotarget.3583>